

NOTICE: This is the author's version of a work that was accepted for publication in [Polymer Testing](#). Changes resulting from the publishing process, such as peer review, editing, corrections, structural formatting, and other quality control mechanisms, may not be reflected in this document. Changes may have been made to this work since it was submitted for publication. A definitive version was subsequently published in [Polymer Testing, Volume 50, April 2016, Pages 73–78](#).

**A novel cup with a pressure-adjusting mechanism for high-temperature water
vapor transmission rate measurements**

Shinya Iizuka ^{a,*}, Kazuhide Murata ^a, Masahiro Sekine ^{b,c}, Chiaki Sato ^d

^a Saitama Industrial Technology Center Northern Laboratory, Saitama, Japan

^b Saitama Industrial Technology Center, Saitama, Japan

^c Institute for High Technology Production Systems, Waseda University, Saitama, Japan

^d Precision and Intelligence Laboratory, Tokyo Institute of Technology, Kanagawa,
Japan

Abstract

Water vapor transmission rate (WVTR) measurements with the conventional cup method do not yield accurate values at high temperatures because the film specimens deform and are damaged owing to air expansion in the cup. A new cup with a pressure-adjusting mechanism allows measurements at 85 °C and prevents specimen deformation and damage. WVTRs of polypropylene (PP) and polyethylene terephthalate (PET) measured with the new cup method are the same as those measured with the conventional cup method at 40 °C, and gas chromatographic detection method at 60 °C and 85 °C. Arrhenius plots of the water vapor permeability coefficient of PP, polyethylene naphthalate (PEN) and polyimide (PI) with the new cup method show a linear relationship in the range 25–85 °C. In the same range, Arrhenius plots of PET, polybutylene terephthalate (PBT) and polylactic acid (PLA) have bending points corresponding to the glass transition temperatures of the materials.

Keywords:

Water vapor transmission rate

Water vapor permeability

Cup method

60 °C 90% RH

85 °C 85% RH

Glass transition temperature

1. Introduction

Proper packaging of electronic components prolongs their life and improves their reliability. To achieve high-performance hermetic packaging, high-barrier materials, such as organic–inorganic hybrid films [1–3] and moisture-proof adhesives [4–7], have been widely developed in recent years.

To develop high-barrier materials, the water vapor barrier properties of such materials have to be understood, especially for electronic components that require high reliability in high-temperature environments [8–10]. However, in the existing standard test methods, there is no reference to high-temperature methods for measuring the WVTR. In contrast, there are references to cup methods [11–14], humidity sensing methods [15–16], infrared detection methods [17–18], electrolytic detection methods [19–20] and gas chromatographic (GC) detection methods [21–22]. For this reason, many material developers rely on their own evaluation methods [23–28].

In 2015, to answer the needs of the industry, ISO adopted new methods for measuring WVTRs of plastics at high-temperature and high-humidity conditions [29–31], e.g., 60 °C and 90% relative humidity (RH) and 85 °C and 85% RH.

The cup method (dish method) in ASTM E96 is a basic standard test method for measuring WVTR. It is simple and inexpensive, and can be used to calibrate the standard test pieces for other methods. However, this method is not suitable for making WVTR measurements at high temperatures because of melting of the sealing wax agent (the typical melting point of wax is approximately 50–60 °C) and the high-temperature deformation and damage of the specimens owing to the increasing internal pressure in the cup.

The purpose of this paper is to present a new, reliable high-temperature cup method using a modified cup that accommodates pressure variations. We verify the validity of the method by performing WVTR measurements of a variety of plastic film samples.

2. Experimental

2.1. Materials

The samples used in this study were PP (OPP bag, WorkUp Co., Ltd.), PET (Lumirror S10, Toray Industries, Inc.), PEN (Teonex Q51, Teijin DuPont Films Japan Ltd.), PI (Mordohar PIF, Future Technology Co., Ltd.), PBT (Smell blocking bag, Kansai Chemicals Co.,Ltd.), and PLA (CF-3S-10P, Lion Office Products Corp.), see abstract for long forms of the abbreviations. Table 1 lists the physical properties of the various film samples. Anhydrous calcium chloride (for U-tube, Wako Pure Chemical Industries, Ltd.) was used as desiccant.

Table 1

Physical properties of various film samples. Asterisk denotes data from ref. [32–34]. Double asterisk indicates $\text{cm}^3(\text{STP})\text{cm}^{-1}\text{s}^{-1}\text{cmHg}^{-1}$ at 35 °C. The gas transition rate was estimated from the thickness of the samples and the gas permeability.

Sample	Thickness [μm]	Glass transition temperature [°C]	Gas permeability*		Gas transition rate	
			[$\text{cm}^3(\text{STP})\text{mm m}^{-2}\text{d}^{-1}\text{atm}^{-1}$]		[$\text{mol m}^{-2}\text{s}^{-1}\text{Pa}^{-1}$]	
			O ₂ (23 °C)	N ₂ (23 °C)	O ₂ (23 °C)	N ₂ (23 °C)
PP	30	-7 *	107	20.5	2×10^{-11}	3×10^{-12}
PET	25	65	0.91	0.2	2×10^{-13}	4×10^{-14}
PEN	25	125 *	0.525	-	1×10^{-13}	-
PI	100	210–270 *	10	2.0	5×10^{-13}	1×10^{-13}
PBT	50	49	15.2	3.04	2×10^{-12}	3×10^{-13}
PLA	125	57	3.36×10^{-11} **	5.40×10^{-12} **	9×10^{-12} (35 °C)	1×10^{-12} (35 °C)

2.2. Test method

WVTR measurements were performed in accordance with the ISO 2528 standard test method. The cup was of screw-type (Imoto Machinery Co., Ltd.), as defined in JIS L 1099 [35]. Anhydrous calcium chloride (desiccant) weighing 20–25 g was placed in the cup. The film specimen was placed on the $\phi 60$ mm cup opening at 3 mm from the desiccant and was fixed by a ring and a screw. The cup was kept in a constant climate cabinet (LHL-113, ESPEC corp.) at a predetermined temperature and 90% RH, and it was taken out at predetermined time intervals and weighed. To ensure airtightness, the cup components were coated with oil compound (HIVAC-G, Shin-Etsu Chemical Co., Ltd.) having high thermo-oxidative stability. The total mass of the cup was weighed after 5–30 min of cooling at room temperature in a desiccator that contained silica gel. The time that the cup was taken out of the climate cabinet is subtracted from the total measuring time. The temperature and humidity in the constant climate cabinet were measured with a HYT-221 sensor (Innovative Sensor Technology, accuracy ± 0.2 °C, $\pm 1.8\%$ RH). The humidity in the cup was determined by a SHTDL-3 miniature humidity sensor (Syscom Corp.) with a HYT-271 sensor element of Innovative Sensor Technology with a low humidity accuracy of $\pm 1\%$ RH. When the cup–desiccant–PET system was kept at 85 °C, 90% RH until 2 g of water vapor permeated, the relative humidity in the cup was maintained under 1.8%.

WVTR ($\text{g m}^{-2}\text{d}^{-1}$) and the water vapor permeability coefficient P ($\text{mol m}^{-1}\text{s}^{-1}\text{Pa}^{-1}$) were calculated using the following equations,

$$\text{WVTR} = \frac{\Delta q}{A\Delta t}$$

$$P = \frac{\Delta q}{A \Delta t} \frac{l}{\Delta p}$$

where $\Delta q/\Delta t$ is the mass change of the cup per time (g d^{-1} or mol s^{-1}), A is the transmission area (m^2), l is the sample thickness (m), and Δp is the difference in partial water vapor pressure between the two sides of the film specimens. Three replicates of each film type were tested.

2.3. Pressure-adjusting mechanism

To prevent specimen deformation and damage owing to the internal pressure variations in the cup, we built a pressure-adjusting gasket and attached it to a conventional cup. The gasket shown in Fig. 1 consists of a polypropylene gasket with side air vents and a laminated aluminum foil bag (HRS-1422S, Meiwa Pax Co., Ltd., the thickness of the Al layer is $9 \mu\text{m}$) for collecting the air leaking from the vents. The gasket was sandwiched between the conventional cup and ring, and coated with oil compound where it overlapped to prevent air leakage. The new cup with the gasket has sufficient air tightness for making WVTR measurements because the measured value for a nonpermeable $30 \mu\text{m}$ thick aluminum sheet is less than $0.2 \text{ g m}^{-2}\text{d}^{-1}$ at $85 \text{ }^\circ\text{C}$ and 90% RH. The new cup was weighed with an electronic balance, and the laminated bag of the gasket was folded over the cup.

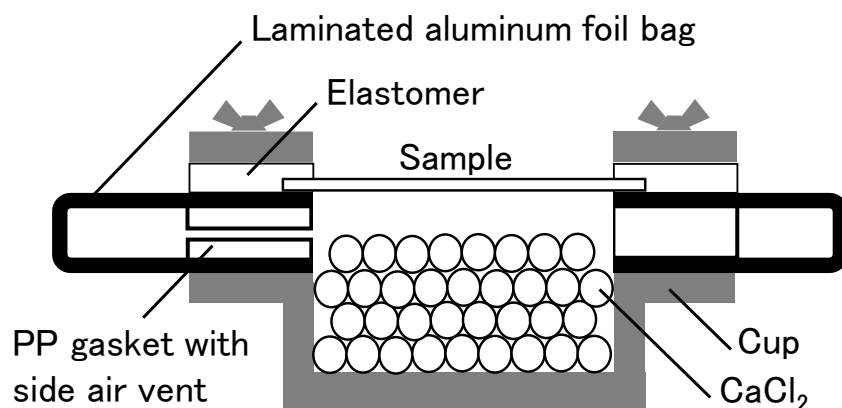


Fig. 1. Schematic of the pressure-adjusting gasket attached on a conventional screw cup

2.4. Pressure measurement in the cup

The air pressure in the conventional cup and the new cup were measured continuously for 24 h at 85 °C and 90% RH by a pressure sensor module (CQ30A-G101, TAISEI Co., Ltd.), which was attached to the cups. Airtightness was maintained.

2.5. WVTR measurements with the GC detection method

WVTR measurements based on the equal pressure method were performed in accordance with ISO 15105-2 using a GC detector sensor (GTR-20FXA, GTR Tec corp.) at 60 °C and 90% RH and 85 °C and 90% RH with a gas flow rate of 30 cc min⁻¹.

2.6. Characterization

The storage modulus E' and loss modulus E'' of each film specimen were investigated during heating at $2\text{ }^{\circ}\text{C min}^{-1}$ at an amplitude of $30\text{ }\mu\text{m}$, frequency of 3 Hz , and temperature range of $25\text{--}85^{\circ}\text{C}$ using a PZ-Rheo NDS-1000 (TAISEI Co., Ltd.). The glass transition temperature of PET, PBT and PLA was determined from the bending of the dynamic viscoelasticity curves with increasing temperature. PBT and PLA were measured without any modification, and PET was measured after the rapid cooling of the melt for removing the internal stresses.

The surface of the film specimens were sputtered with gold and observed using a JSM-IT300LA scanning electron microscope, operating at an accelerating voltage of 15.0 kV .

3. Results and discussion

3.1. WVTR measurement of plastic films

Table 2 shows the WVTRs of PP and PET at several temperatures measured with the conventional cup method, the new cup method and the GC detection method at 60 °C and 85 °C.

Table 2

WVTRs of PP and PET at a predetermined temperature and 90% RH.

Sample	Condition	WVTR [$\text{g m}^{-2}\text{d}^{-1}$]		
		Conventional cup method	New cup method	GC detection method
PP	40 °C, 90% RH	5.0	5.0	-
	60 °C, 90% RH	23.1	23.6	22.9
	85 °C, 90% RH	179	136	133
PET	40 °C, 90% RH	26.1	25.9	-
	60 °C, 90% RH	79.1	74.9	73.2
	85 °C, 90% RH	302	273	269

At 40 °C and 60 °C, the results for PP are the same for both the new cup and the conventional cup method; however, at 85 °C, the WVTR for PP by the new cup method is 24% lower. In the case of PET, the results with the new cup method are the same at 40 °C, 5% lower at 60 °C, and 9% lower at 85 °C. In both samples, the results for the

new cup method at 60 °C and 85 °C are within 3% of the results with the GC detection method. The GC detection method is capable of measuring WVTR without any deformation or damage to the specimens at high temperatures because both specimen sides are at equal pressures. The results show that the WVTR values produced by the new cup method are comparable to those produced by the GC detection method at 60 °C and 85 °C.

The conventional cup method for PP and PET has different sources of errors at high temperatures. The PP film is concave, as shown in Fig. 2, after measuring WVTR at 85 °C. The film is in close contact with the calcium chloride and damage is observed on the surface, as shown in Fig. 3. The concave PP film measured at 60 °C does not make contact with the calcium chloride and no damage is observed. Also, no damage is observed in the PET films at 60 °C and 85 °C.



Fig. 2. Top view photograph of the PP film on a conventional screw-type cup after measuring WVTR at 85 °C.

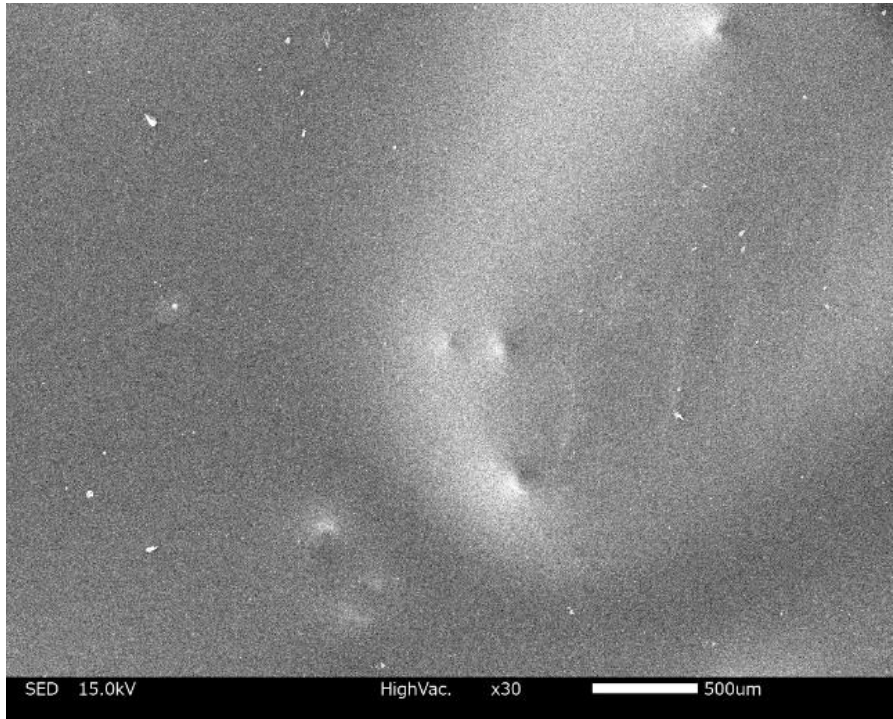


Fig. 3. Scanning electron microscope image of the PP film after measuring WVTR at 85 °C by the conventional cup method. A magnification of figure is 30×.

Figure 4 shows the shape change of PP and PET after the WVTR measurements at 85 °C and 90% RH using the conventional cup and the new cup method. In the case of the conventional cup method, PP and PET have convex shape after heating at 85 °C. When held for 24 h at 85 °C, the PP shape returns to horizontal, whereas PET remains inflated. After cooling, PP is dented and PET is bent. In contrast, both PP and PET maintained their initial state in the new cup method during the WVTR measurements. The laminated bag of the gasket inflates during heating, which, after being held for 24 h at high temperatures, shrinks for PP and remains inflated for PET.

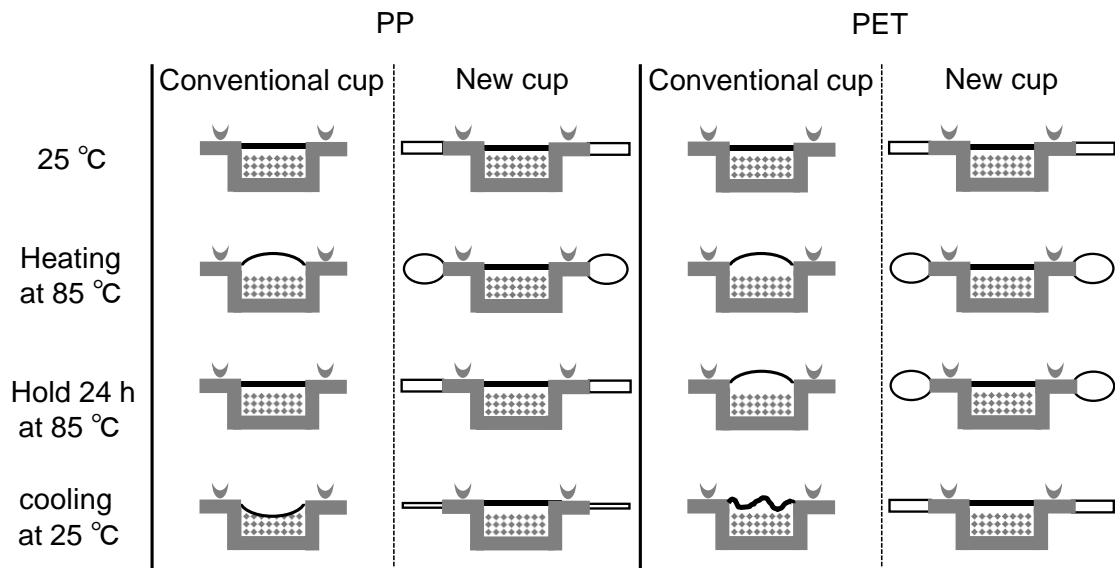


Fig. 4. Schematic of the shape change of PP and PET during the WVTR measurements.

Figure 5 shows the air pressure in each cup in Fig. 4 when heated at 85 °C for 24 h. In the case of the conventional cup, air pressure increased to about 5–7 kPa after heating and then gradually decreased; it returned to the atmospheric value in about 8 h for PP, and to 2.5 kPa after 24 h for PET.

It seems reasonable to assume that the pressure in the cups decreased because of air (O_2 and N_2) permeance. The air transmission rate for PP is higher than that for PET (Table 1) and the air in the cup is speedily transmitted through PP; thus, the pressure difference at each side of PP is also quickly eliminated. Upon cooling, the air pressure in the cup is lower than the atmospheric pressure and, consequently, PP becomes concave. Conversely, the air in the cup in PET measurements is hard to permeate to the outside and, subsequently, the pressure in the cup is nearly atmospheric after cooling. Clearly, the shape changes of PP affect the WVTR measurements. Presumably, the

conventional cup method gives results that are greater than the results of the GC detection method. In the new cup method, the expanded air in the cup owing to heating escapes to the laminated bag of the pressure-adjusting gasket. Accordingly, the air pressure hardly changes and the film shape does not change. The results of the new cup method and the GC detection method are about the same.

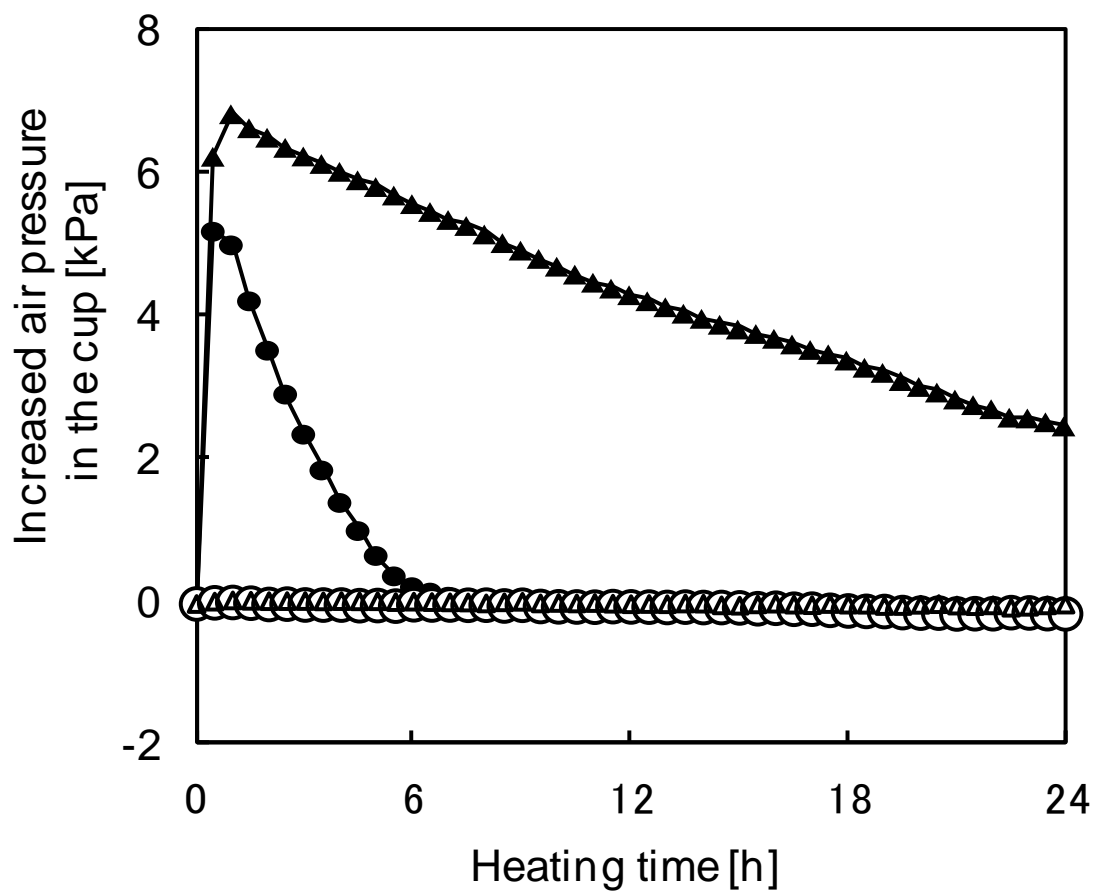


Fig. 5. Air pressure vs time during WVTR measurements at 85 °C with the conventional cup method (●: PP, ▲: PET) and the new cup method (○: PP, △: PET)

3.2. Temperature dependence of the water vapor permeability

Figure 6 shows the temperature dependence of P for PP measured with the conventional cup and the new cup method. The same linear relationship is seen in the range 25–85 °C for the new cup method and in the range 25–60 °C for the conventional cup method. The two methods start to deviate at ≥ 70 °C.

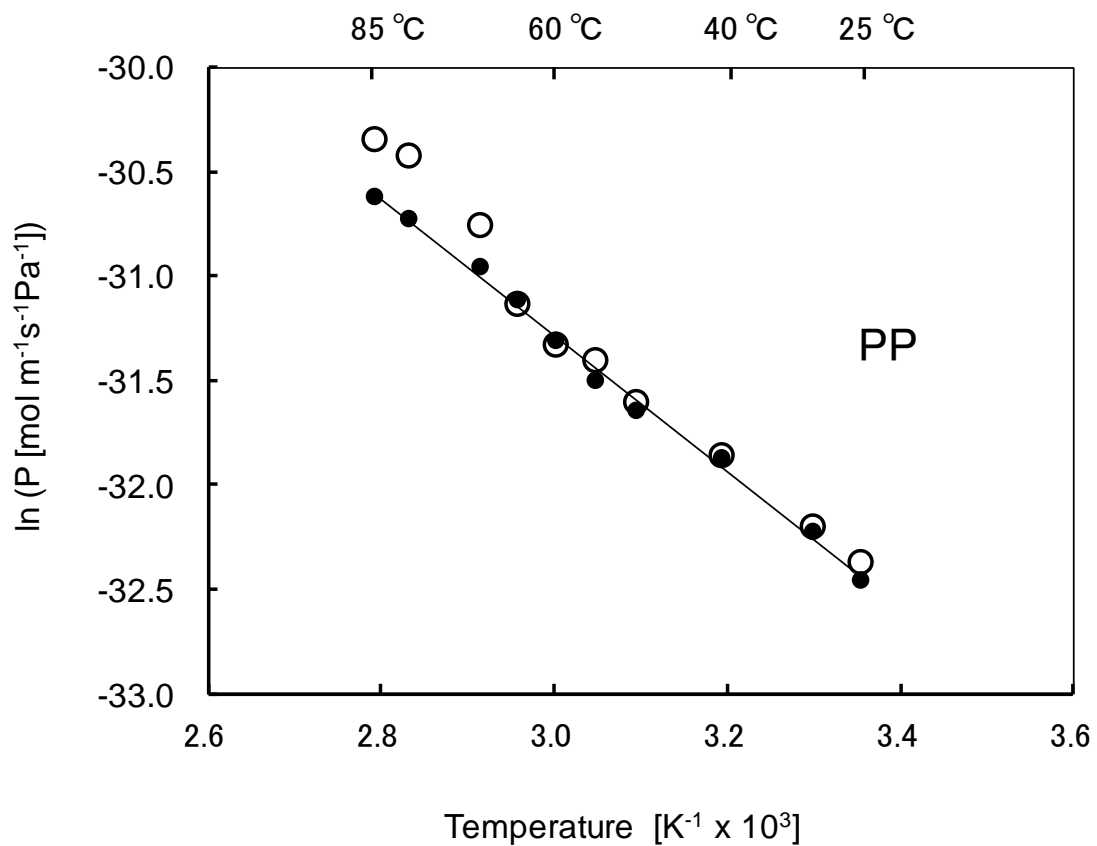


Fig. 6. Arrhenius plots of P for the PP film measured by the conventional cup method (○) and the new cup method (●).

The water vapor permeability of the typical polymer films can be described by an Arrhenius-type equation. The measurement results with the new cup method are consistent with the previous result for PP [36], which is stable in this temperature range. The higher P values at ≥ 70 °C with the conventional cup method are attributed to film deformation and damage, as discussed above.

Figure 7 shows the temperature dependence of P for PEN and PI, which are stable in this temperature range. Linear relationships between P and temperature are seen for PEN and PI in the range 25–85 °C with the new cup method and 25–70 °C with the conventional cup method. The results of the conventional cup method at 85 °C are slightly above the results of the new cup method. Comparing WVTR at 85 °C, we find differences of 8% in PEN and 3% in PI. These are smaller than the difference of 24% in PP (Table 2). PEN and PI have lower air permeability than PP (Table 1); thus, they acquire a convex shape after the WVTR measurements with the conventional cup method. The convex shape suggests that the differences described above are probably caused by an increase in the transmission area that is associated with film swelling. The storage modulus E' of PP, PEN, and PI at 85 °C is 0.3 GPa, 2.5 GPa, and 1.1 GPa, respectively, and the film thicknesses are shown in Table 1. These physical properties lead to differences in the degree of bulging owing to the increase in internal pressure, and seem to affect the measurements.

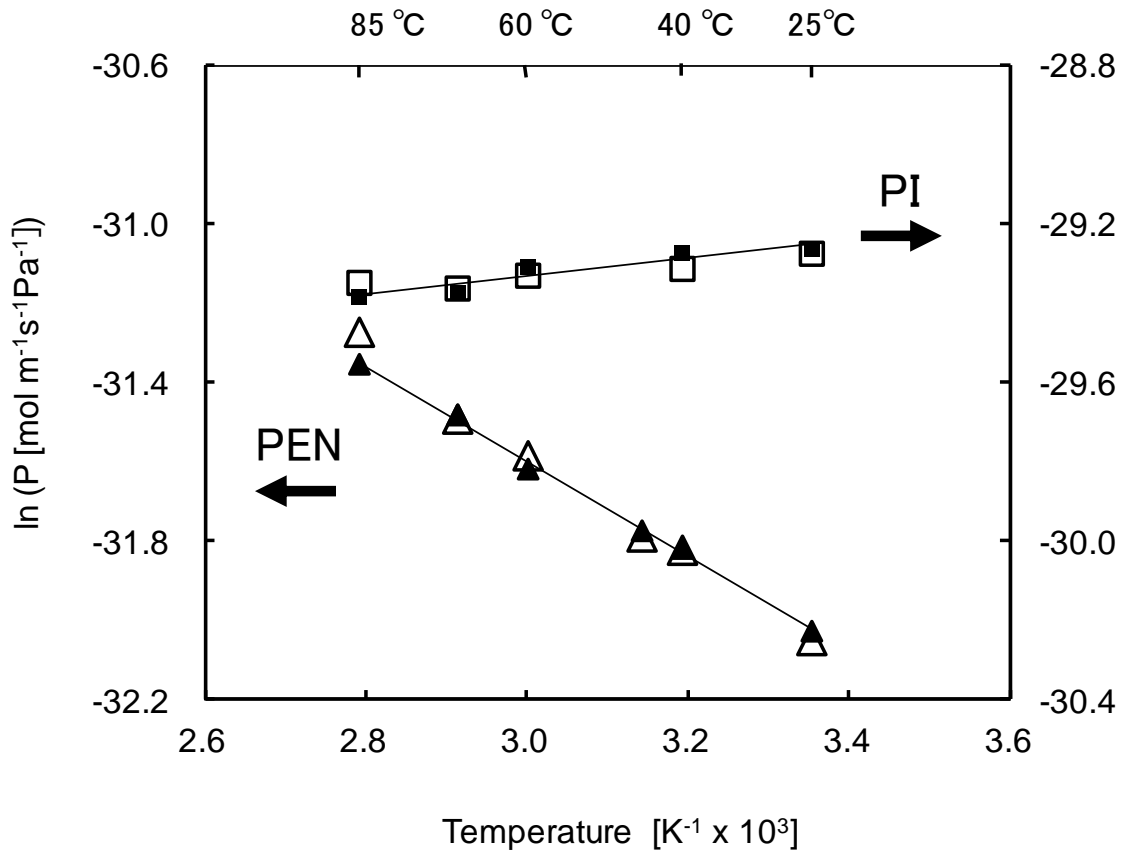


Fig. 7. Arrhenius plots of P for PEN and PI films measured by the conventional cup method (\triangle , \square) and the new cup method (\blacktriangle , \blacksquare).

3.3. The change of water vapor permeability

Figure 8 shows the temperature dependence of P for PET measured by the conventional cup method and the new cup method. In the case of the conventional cup method, P varies widely and the slope does not clearly point to a bending point. In contrast, in the case of the new cup method, P values fall on two lines that intersect at about 60 °C.

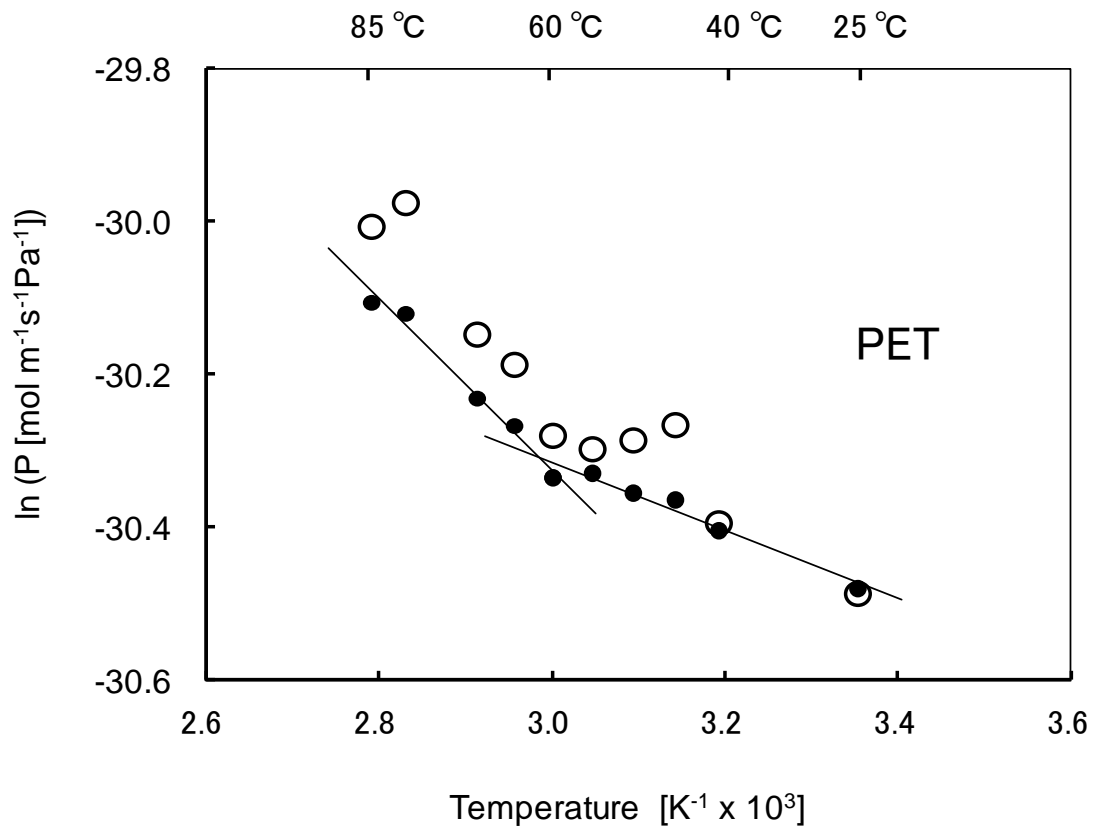


Fig. 8. Arrhenius plots of P values of PET film measured by a conventional cup method (○) and the new cup method (●).

Figure 9 shows the temperature dependence of P for PBT and PLA. At 85 °C, PLA cracks and PBT deforms during the conventional cup method and the measurement results clearly show modulation at 85 °C. On the contrary, the new cup method does not damage or deform the films, and clearly shows bending points in the P values as with PET.

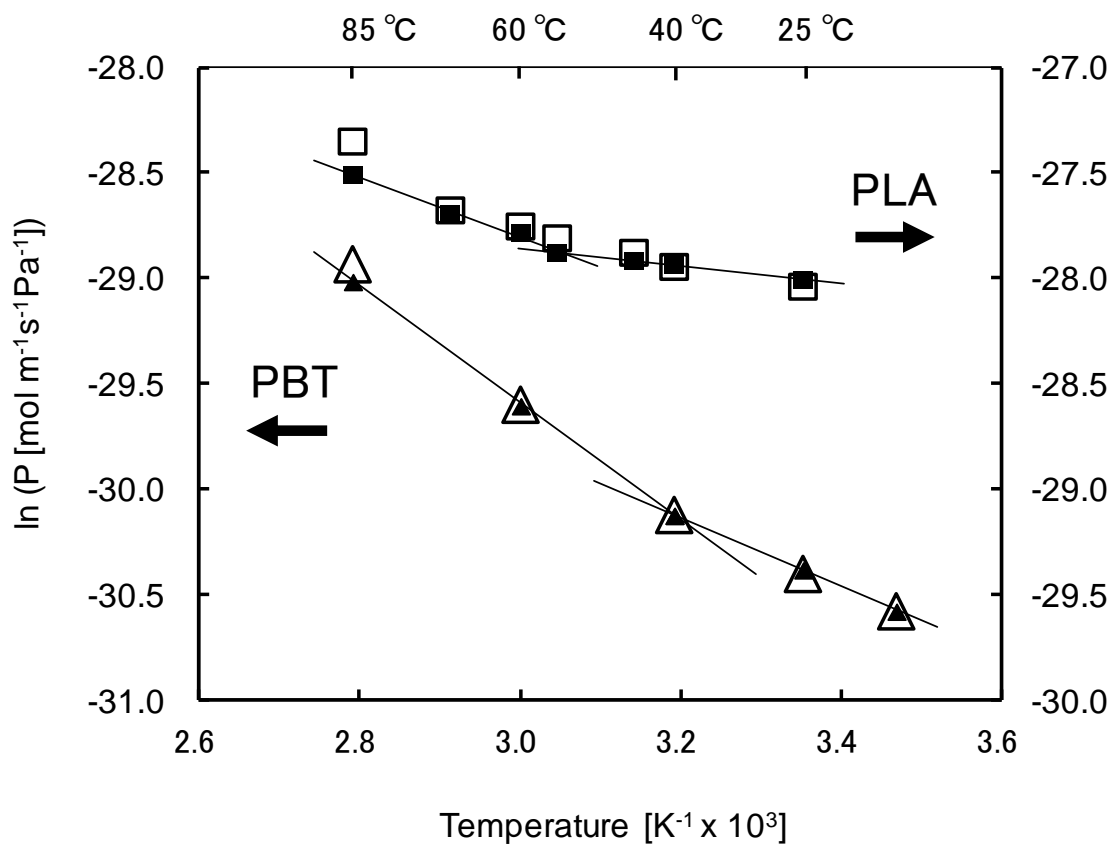


Fig. 9. Arrhenius plots of P for PBT and PLA films measured with the conventional cup method (\triangle , \square) and the new cup method (\blacktriangle , \blacksquare). A low-temperature and humidity chamber (PL-2KPH) is used at 15 °C ($3.47 \times 10^{-3} K^{-1}$).

3.4. Characterization

It is clear that damage to the specimen in the high-temperature range (such as with PP shown in Fig. 3) caused an increase in the water vapor permeability. PLA also cracked, resulting in a significantly larger WVTR than that obtained by the new cup method (Fig. 9).

Meanwhile, the bending points of PET, PBT, and PLA were not caused by damage or deformation of the specimen. A. Launay [37] reported that the bending point of P values for PET appears at 60–80 °C and corresponds to the glass transition of PET. The temperature of the bending point shown in Figs. 8 and 9 is almost consistent with the glass transition temperature of the specimen, shown in Table 1. We conclude that the new cup method may be used to detect structural changes in materials according to the glass transition.

Because the new cup method prevents damage to the specimen in the high-temperature range, it is suitable for measuring a fragile thin layer coated on the film and for evaluating materials that have a glass transition temperature in the range of 25–85 °C, such as epoxy resin adhesives.

4. Conclusions

At high-temperature conditions, WVTR values with the conventional cup method are higher than those obtained with the GC detection method because of specimen deformation and damage owing to pressure fluctuations in the cup. A new cup fitted with a pressure-adjusting gasket eliminates the pressure fluctuations. At 60 °C and 85 °C, the results with the new cup method are the same as those with the GC detection sensor method. Arrhenius plots of P values for PP, PEN and PI using the new cup method show a linear relationship at 25–85 °C because the samples are stable in this temperature range. Arrhenius plots of P values for PET, PBT, and PLA with the new cup method identify bending points that correspond to the glass transition temperatures of the materials.

References

1. [P. E. Burrows, G. L. Graff, M. E. Gross, P. M. Martin, M. K. Shi, M. Hall, E. Mast, C. Bonham, W. Bennett, M. B. Sullivan, Display 22 \(2001\) 65–69.](#)
2. [G. L. Graff, R. E. Williford, P. E. Burrows, J. Appl. Phys. 96, \(2004\) 1840–1849.](#)
3. [K. Saitoh, R. S. Kumar, S. Chua, A. Masuda, H. Matsumura, Thin Solid Films 516 \(2008\) 607–610.](#)
4. [R. Doerfler, S. Barth, C. Boeffel, A. Wedel, SID Symposium Digest of Technical Papers 37 \(2006\) 440–443.](#)
5. [M. A. Osman, V. Mittal, M. Morbidelli, U. W. Suter, Macromolecules 36 \(2003\) 9851–9858.](#)
6. [C. E. Corcione, P. Prinari, D. Cannoletta, G. Mensitieri, A. Maffezzoli, Int. J. Adhesion and Adhesives 28 \(2008\) 91–100.](#)
7. [J. K. Kim, C. Hu, R. S. C. Woo, M. L. Sham, Composites Science and Technology 65 \(2005\) 805–813.](#)
8. EIAJ ED-4701/100 Environmental and endurance test methods for semiconductor devices (Life test I).
9. IEC 60068-2-67 Environmental testing - Part 2-67: Tests - Test Cy: Damp heat, steady state, accelerated test primarily intended for components.
10. MIL-STD-810 Method 507.3 Temperature Humidity Bias.
11. ISO 2528 Sheet materials - Determination of water vapour transmission rate - Gravimetric (dish) method.
12. ASTM E 96 Standard Test Methods for Water Vapor Transmission of Materials.
13. JIS Z 0208 Dish Method: Testing Methods for Determination of the Water Vapor

Transmission Rate of Moisture-Proof Packaging Materials.

14. DIN 53122-1 Testing of plastics and elastomer films, paper, board and other sheet materials - Determination of water vapour transmission - Part 1: Gravimetric method.

15. ISO 15106-1 Plastics - Film and sheeting - Determination of water vapour transmission rate - Part 1: Humidity detection sensor method.

16. ASTM E398 Standard Test Method for Water Vapor Transmission Rate of Sheet Materials Using Dynamic Relative Humidity Measurement.

17. ISO 15106-2 Plastics - Film and sheeting - Determination of water vapour transmission rate - Part 2: Infrared detection sensor method.

18. ASTM F 1249 Standard Test Method for Water Vapor Transmission Rate Through Plastic Film and Sheetting Using a Modulated Infrared Sensor.

19. ISO 15106-3 Plastics - Film and sheeting - Determination of water vapour transmission rate - Part 3: Electrolytic detection sensor method.

20. DIN 53122-2 Determination of water vapour transmission (density of moisture flow rate) of plastic films, elastomer films, paper, board and other sheet materials; electrolysis method.

21. ISO 15106-4 Plastics - Film and sheeting - Determination of water vapour transmission rate - Part 4: Gas-chromatographic detection sensor method.

22. JIS K 7129-C Plastics - Film and sheeting - Determination of water vapour transmission rate - Instrumental method (Appendix C Gas-chromatographic detection sensor method).

23. [P. F. Carcia, R. S. McLean, M. H. Reilly, M. D. Groner, S.M. George, Appl. Phys. Lett. 89 \(2006\) 031915.](#)

24. [P. Hülsmann, D. Philipp, M. Köhl, Rev. Sci. Instrum. 80 \(2009\) 113901.](#)

25. [M. O. Reese, A. A. Dameron, M. D. Kempe, Rev. Sci. Instrum. 82 \(2011\) 085101.](#)
26. [G. J. Jorgensen, K. M. Terwilliger, J. A. DelCueto, S. H. Glick, M. D. Kempe, J. W. Pankow, F. J. Pern, T. J. McMahon, Sol. Energ. Mat. Sol. C. 90 \(2006\) 2739–2775.](#)
27. [G. Jorgensen, K. Terwilliger, S. Glick, J. Pern, T. McMahon, the National Center for Photovoltaics and Solar Program Review Meeting \(2003\).](#)
28. [J. A. Hauch, P. Schilinsky, S. A. Choulis S. Rajoelson, C. J. Brabec, App. Phys. Lett. 93 \(2008\) 103306.](#)
29. ISO 15106-5 Plastics - Film and sheeting - Determination of water vapour transmission rate - Part 5: Pressure sensor method.
30. ISO 15106-6 Plastics - Film and sheeting - Determination of water vapour transmission rate - Part 6: Atmospheric pressure ionization mass spectrometer method.
31. ISO 15106-7 Plastics - Film and sheeting - Determination of water vapour transmission rate - Part 7: Calcium corrosion method.
32. [Encyclopedia of Polymer Science and Technology, Wiley Online Library.](#)
33. [L. W. McKeen, Permeability properties of plastics and elastomers. Second ed., Plastics Design Library, New York \(2003\).](#)
34. [T. Komatsuka, A. Kusakabe, K. Nagai, Desalination 234 \(2008\) 212–220.](#)
35. JIS L 1099 Testing methods for water vapour permeability of textiles.
36. [Paul M. Doty, W. H. Aiken, H. Mark, Ind. Eng. Chem. 38 \(1946\) 788–791.](#)
37. [A. Launay, F. Thominette, J. Verdu, J. Appl. Polym. Sci. 73 \(1999\) 1131–1137.](#)